Design Optimization of Additively Manufactured HFIR Control Elements

J. R. Burns,[1] D. Chandler,[1] B. Petrovic[2]

[1]*Oak Ridge National Laboratory, Oak Ridge, TN 37831*
[2]*Georgia Institute of Technology, Atlanta, GA 30332*
burnsjr@ornl.gov

INTRODUCTION

The High Flux Isotope Reactor (HFIR) at Oak Ridge National Laboratory provides one of the highest steady-state neutron sources in the world for use across a broad range of research activities, including neutron scattering, isotope production, and activation analysis [1]. HFIR's two control elements (CEs) are essential reactor operation and safety components which must be regularly replaced as irradiation damage accumulates. However, the current fabrication process for the HFIR CEs is highly time-consuming and expensive [2]. In light of this, the ultrasonic additive manufacturing (UAM) process [3] is under investigation for application to HFIR CE fabrication, offering potential to simplify the process and yield significant savings in the associated cost, time, and labor.

UAM yields a novel CE design with discretized regions of neutron-absorbing material, in contrast to a traditional CE design with uniformly distributed absorbers [4]. Fig. 1 compares a cross section of each CE design highlighting the differences. This design change not only impacts the neutronic characteristics of the HFIR CEs, but also introduces new design variables that were not applicable to the original CE design. Previous work has verified the neutronic and operational feasibility of employing the discrete CE design in HFIR, demonstrating comparable performance throughout the CE useful lifetime [5, 6]. This study seeks to take advantage of the expanded design space to optimize the discrete CE design. As HFIR is a well-established research reactor with decades of operating experience, it is desired to avoid detailed reevaluation of the existing HFIR safety margins upon introduction of the new CEs. Thus, the discrete CEs are to be designed to minimize their impact on the HFIR core physics, ensuring compliance with the established safety envelope. This high-level objective forms the foundation of the optimization problem investigated here.

Fig. 1. CE design comparison

HFIR Core Design Overview

HFIR is a flux trap-type light water-cooled research reactor operating nominally at 85 MWt [1]. The HFIR core comprises several distinct concentric annular regions, as illustrated in Fig. 2 [2]. In the center of the core is the flux trap region, with dozens of experimental facilities surrounded by moderating water to enable irradiation at peak thermal fluxes on the order of 10^{15} n/cm^2-s. The flux trap extends to a radius of roughly 6 cm. Two fuel elements, an inner fuel element (IFE) and an outer fuel element (OFE), surround the flux trap. Each fuel element is roughly 7 cm thick and is loaded with hundreds of 93% enriched U_3O_8-Al fuel plates roughly 1 mm in thickness.

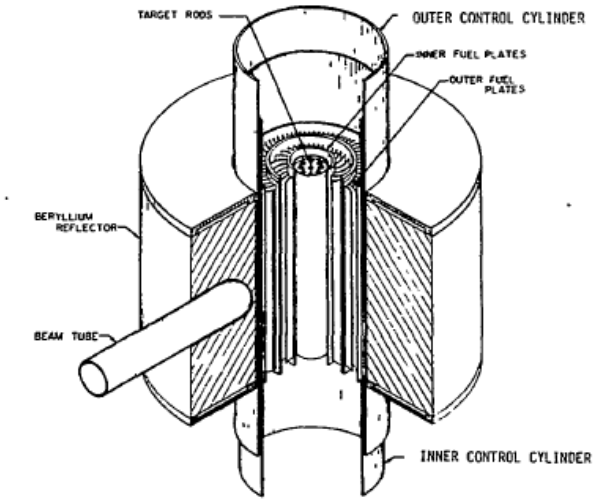

Fig. 2. HFIR core schematic [2]

The two CEs, an inner CE (ICE) and an outer CE (OCE), each 0.635 cm thick, surround the fuel elements. Each CE comprises three axial regions of varying neutron absorption opacity: the white regions contain only structural aluminum and do not contribute to absorption; the gray regions contain Ta as the primary absorber in a concentration of 30% by volume; and the black regions contain Eu as the primary absorber in the form of Eu_2O_3 with a concentration of 33% by volume. The absorbing CE regions are gradually withdrawn vertically from the core during operation to maintain criticality as the fuel

depletes. A beryllium reflector 30 cm thick is the final core component surrounding the CEs.

DESCRIPTION OF WORK

Optimization Problem Formulation

In the original CE design with uniformly distributed absorbers, the only design variables are the absorber concentrations in the gray and black regions. By discretizing the neutron absorbers into individual compacts arranged in a regular cylindrically symmetric array [5], the azimuthal spacing between compacts, compact size, and absorber concentrations in the compacts can all be varied. The design space for the discrete CEs is therefore defined as follows:

$$\boldsymbol{x} = \langle s_{ig}, s_{ib}, s_{og}, s_{ob}, r, t, a_g, a_b \rangle \qquad (1)$$

where **x** is the position vector identifying the point in design space, s is the angular spacing between adjacent absorber compacts, r is the compact radius, t is the compact thickness, a is the absorber concentration in the compacts, the subscript "i" refers to the ICE, the subscript "o" refers to the OCE, the subscript "g" refers to the gray regions, and the subscript "b" refers to the black regions. The initial settings of the discrete CE design variables are given in Table I; these settings were selected to match the absorber mass content of each absorbing region of the homogeneous CEs [5].

TABLE I. Initial Discrete CE Design

Design Variable	Value
s_{ig}	0.028516 rad
s_{ib}	0.027660 rad
s_{og}	0.027921 rad
s_{ob}	0.027128 rad
r	0.2795 cm
t	0.171 cm
a_g	90 w/o Ta
a_b	81.5 w/o Eu_2O_3

Compliance with the existing HFIR safety margins can be guaranteed if the core power distribution with discrete CEs is the same as that with the original homogeneous CEs; this would maintain core outlet temperatures and ensure reliable core cooling. The objective quantity is therefore defined as:

$$f(\boldsymbol{x}) = \sum_i (\Delta RFD_i)^2 \qquad (2)$$

where f is the objective value, **x** is the position vector in design space as defined previously, ΔRFD_i is the difference in relative fission density at a core location i, and the summation is taken over all points of a cylindrical mesh imposed over the core. The value of f defined in this way represents the L2 distance between the core power distribution under the original homogeneous CEs and that with discrete CEs, providing a suitable minimization objective in the following optimization procedure.

The optimization search must be constrained by some practical considerations. For structural integrity, separation must be maintained between absorber compacts in all regions:

$$s_{ig}, s_{ib}, s_{og}, s_{ob} > 0 \qquad (3)$$

The discrete CE design also must not truncate the HFIR cycle length. This can be ensured by requiring that core reactivity is at least the same as with the homogeneous CEs:

$$k \geq k_{hom} \qquad (4)$$

where k is the neutron multiplication eigenvalue under a CE design and the subscript "hom" refers to the homogeneous CEs. The neutron multiplication eigenvalue under the homogeneous CEs is 1.00829.

Finally, consideration of CE reactivity worth provides a soft constraint. There is no hard minimum reactivity worth requirement as long as the CEs provide acceptable shutdown margin. Thus, upon identification of an optimal design, it must be verified that it exhibits reactivity worth comparable to the original CEs.

Optimization Methodology

A deterministic optimization approach is sought due to the computational rigor of the HFIR models used for transport calculations [6] precluding a stochastic approach. Deterministic methods typically require a mathematical formulation of the relationship between the objective and constraints and the decision (design) variables; however, no such closed-form mathematical description is available in this application. Though the Boltzmann transport equation theoretically provides the basis for such a relationship, the core power distribution and neutron multiplication eigenvalue can only be practically calculated via explicit transport simulations with MCNP5 [7]. Therefore, response surface methodology (RSM) [8-10] is employed to statistically infer the mathematical relationship between the objective and the eigenvalue and the design variables.

RSM is commonly employed in applications where simulation or experimentation is required to measure the response of a system to perturbations [8-12]. In this study, RSM is used to fit (via least squares regression) second-order response surfaces representing the objective and the neutron multiplication to a limited set of local perturbed designs evaluated with MCNP5 under beginning of cycle

(BOC) conditions. These perturbations are selected to minimize confounding of design variable effects [8-11]. A local minimum in the objective response surface is then sought without violating the eigenvalue constraint. The optimization search remains local, as a global search would require evaluating points in the design space far from the initial settings; the details of actually fabricating such divergent designs (e.g., very large absorber compacts that would be affected by curvature) are not yet well understood.

RESULTS

The objective value corresponding to the initial design is 0.019058, and the neutron multiplication eigenvalue is 1.00961 (the initial design therefore satisfies the cycle length constraint and is feasible). The optimal design settings identified using RSM are listed in Table II, along with the corresponding objective value and neutron multiplication eigenvalue. The optimal design was found to be located very near in design space to the initial design and yielded a small but nontrivial improvement in the objective value. This is likely a consequence of closely matching the discrete CE absorber content to that of the homogeneous CEs, while remaining discrepancies are inherent limitations of employing discretized absorbers.

TABLE II. Optimal Discrete CE Design

Variable	Value
s_{ig}	0.028325 rad
s_{ib}	0.027669 rad
s_{og}	0.027937 rad
s_{ob}	0.026574 rad
r	0.28118 cm
t	0.17241 cm
a_g	90.2965 w/o Ta
a_b	81.9078 w/o Eu_2O_3
Objective f	0.018528
Eigenvalue k	1.00853

For a more detailed assessment of the improvement in the power distribution yielded by the optimal design, Fig. 3 plots the shift in relative power density introduced by the initial discrete CE design relative to the homogeneous CEs in the r-z plane as well as the corresponding uncertainty; Fig. 4 gives the same for the optimal design. The initial discrete CE design introduces a slight radially outward shift in the power distribution that is limited to within 2%. The optimal design largely succeeds in correcting this, but the correction is nonuniform and is excessive at some points and lacking at others. Some improvement was achieved nonetheless, and the remaining differences are not expected to violate the established thermal margins. Further improvements could be realized by assessing additional design perturbations about this point and fitting new response surfaces, but this is not considered necessary, as it was found that perturbations of each design variable in either direction yielded an increase in the objective value.

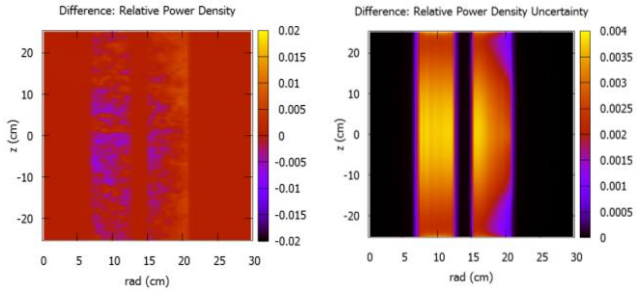

Fig. 3. Shift in relative power density introduced by initial discrete CE design relative to homogeneous CE design

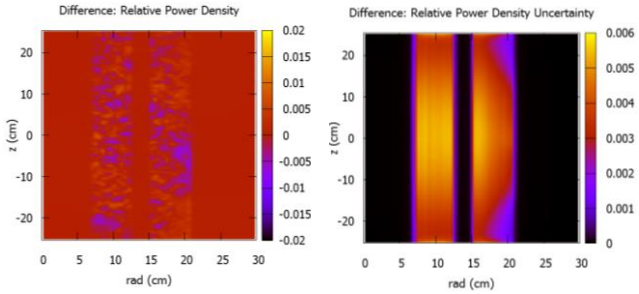

Fig. 4. Shift in relative power density introduced by optimal CE design relative to homogeneous CE design

Finally, the differential and integral reactivity worth of the optimal CE design at the nominal BOC CE position [1] are calculated for comparison against the homogeneous CEs as well as the initial discrete CE design. The BOC CE position of the homogeneous CEs is applied to both discrete designs. These reactivity worth results are presented in Table III. The initial discrete CE design maintains both differential and integral reactivity worth that are comparable to and indeed exceed those of the homogeneous CEs. This remains the case with the optimal design, thereby guaranteeing acceptable shutdown margin.

TABLE III. Reactivity Worth Comparison

Design	Diff. Worth (¢/cm)	Int. Worth (¢)
Optimal	104.5 ± 0.7	1412 ± 2
Initial Discrete	103.9 ± 1.6	1414 ± 3
Homogeneous	102.8 ± 1.6	1407 ± 3

CONCLUSIONS

The design of additively manufactured HFIR CEs with discretized neutron absorbers has been optimized to minimize their impact on the HFIR core power distribution, thus maintaining compliance with established thermal safety margins and avoiding rigorous reevaluation of HFIR safety analyses. RSM was employed to facilitate the optimization search by statistically inferring the mathematical relationship between the objective and constraining parameters and the design variables. It was verified that the optimized CE design does not introduce large shifts in the core power distribution that would challenge reactor safety, nor does it sacrifice reactivity worth. It is therefore concluded that this optimized CE design is feasible for use in the operation of HFIR while providing as seamless of a transition as possible in implementing the new design.

Complementary to [5] and [6], this study rounds out the neutronic feasibility assessment of additively manufactured CEs in HFIR; however, the practical implementation of additively manufactured CEs in HFIR requires additional analyses and testing. Immediate next steps include thermal-hydraulic analyses to verify adequate cooling of both the core and the CEs under existing systems; transient analyses to assess the performance of the additively manufactured CEs under postulated accident conditions; and mechanical and irradiation testing of physical samples of the additively manufactured CEs to determine the CE integrity in the HFIR core environment. The UAM method itself is also the subject of active research on process improvements [13, 14] with significant implications for the mechanical and material characteristics of the components studied here. The results of these studies in conjunction with the neutronics results presented in this work are promising, instilling enthusiasm for the potential economic benefits offered by employing UAM in the fabrication of HFIR CEs as well as the possibility of expanding its application elsewhere in the nuclear industry.

ACKNOWLEDGMENTS

The technical review of Joshua Peterson-Droogh at ORNL is gratefully acknowledged. This research was carried out using Laboratory-Directed R&D funding at ORNL.

REFERENCES

1. G. ILAS et al., “Modeling and Simulations for the High Flux Isotope Reactor Cycle 400,” ORNL/TM-2015/36, Oak Ridge National Laboratory (2015).
2. J.D. SEASE, “Fabrication of Control Rods for the High Flux Isotope Reactor,” ORNL/TM-9365/R1, Oak Ridge National Laboratory (1998).
3. R.J. FRIEL and R.A. HARRIS, “Ultrasonic Additive Manufacturing – A Hybrid Production Process for Novel Functional Products,” Procedia CIRP 6 (2013) 35-40.
4. K. TERRANI et al., “Demonstration of Advanced Manufacturing Techniques for Production of Nuclear Core Structures: Ultrasonic Additive Manufacturing of Hybrid Structures Resembling HFIR Control Plates,” *Transactions of the American Nuclear Society* (June 2015).
5. J. BURNS et al., “Reactor Physics Phenomena in Additively Manufactured Control Elements for the High Flux Isotope Reactor,” *Annals of Nuclear Energy* 115 (2018) 403-414.
6. J. BURNS et al., “Depletion and Lifetime Performance Analysis of Advanced Manufactured Control Elements in the High Flux Isotope Reactor,” *Proc. ICAPP 2018*, Charlotte, NC, April 8-11 2018, submitted (2018).
7. X-5 MONTE CARLO TEAM, “MCNP – A General Monte Carlo N-Particle Transport Code, Version 5.” LA-UR-03-1987, Los Alamos National Laboratory (2003).
8. G.E.P. BOX et al., *Statistics for Experimenters*, pp. 510-537. New York: John Wiley & Sons (1978).
9. “Response Surface Methodology Handbook for Nuclear Reactor Safety,” EUR-9600 EN, Commission of the European Communities (1984).
10. H.G. NEDDERMEIJER et al., “A Framework for Response Surface Methodology for Simulation Optimization.” *Proceedings – Winter Simulation Conference*, Orlando, FL, December 10-13, 2000.
11. V.L. ANDRESON and R.A. MCLEAN, *Design of Experiments: A Realistic Approach*, pp. 225-278. Marcel Dekker, Inc. (1974).
12. U. KIM and P. SEONG, “Optimization of the Worth Shape of Axially Variable Strength Control Rods with Simulation Optimization Methodology for the Power Maneuvering of Pressurized Water Reactors.” *Nuclear Engineering and Design* 225 (2003) 27-35.
13. M.N. GUSSEV et al., “Effect of Post Weld Heat Treatment on the 6061 Aluminum Alloy Produced by Ultrasonic Additive Manufacturing.” *Materials Science and Engineering A* 684 (2017) 606-616.
14. P.J. WOLCOTT et al., “Process Improvements and Characterization of Ultrasonic Additive Manufactured Structures.” *Journal of Materials Processing Technology* 233 (2016) 44-52.